Journal of Loss Prevention in the Process Industries 76 (2022) 104750

Contents lists available at ScienceDirect

Journal of Loss Prevention in the Process Industries

journal homepage: www.elsevier.com/locate/jlp

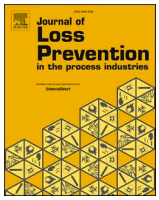

Influence of wind speed and ammonia concentration on its evaporation rate from aqueous solution spills

Agustín Corruchaga [a], Oriol Casal [b], Adriana Palacios [c], Joaquim Casal [a,*]

[a] Center for Technological Risk Studies (CERTEC), Chemical Engineering Department, Universitat Politècnica de Catalunya. Barcelona, Catalonia, Spain
[b] Chemical Engineering Department, Universitat Politècnica de Catalunya. Barcelona, Catalonia, Spain
[c] Universidad de Las Americas Puebla, Department of Chemical, Food and Environmental Engineering, Puebla, Mexico

ARTICLE INFO

Keywords:
Aqueous solution spills
Ammonia evaporation rate
Wind speed influence
Mathematical modeling

ABSTRACT

In the event of an accidental spill of an aqueous solution of ammonia, a toxic cloud can be generated, being the ammonia evaporation rate a key issue. In this communication, new experimental data have been obtained at different initial ammonia concentrations and air speeds. The evolution of the evaporation rate, of the ammonia concentration in the solution and of the solution temperature have been studied. Three phases have been clearly identified in the evaporation process, affected by the ammonia concentration, the evaporation rate and the condensation of water. A simple model has also been proposed, based on previous ones from the literature and now including the condensation of water. The proposed model has been compared with experimental data. Although some scattering has been found, it still proves itself useful at predicting the source term in the event of an accidental spill.

1. Introduction

A high number of research papers have been published on the risks associated with liquid hydrocarbon spillages, in either process plants, storage or transportation. Most of them deal with their flammability properties, which make them prone to fires or explosions. Nevertheless, in some cases other chemicals are released, also implying a risk. Depending on their properties, the toxicity of the substance can imply notorious negative consequences. Historical accidents surveys show that besides the possible fatalities, toxic clouds originate 4.5 times more injured people than fires and 2.5 more than explosions (Ronza et al., 2006). A recent historical survey (Toscano et al., 2022) on pipeline transportation of ammonia identified 136 accidents in which this chemical was spilled. In an important number of them, the evaporation led to the formation of a toxic cloud with potential risk for the population; in the Kingman (Kansas) accident, occurred in 2004, for example, the 1% lethality isopleth as estimated by these authors reached a distance of approximately 600 m.

Ammonia can be released as an aqueous solution or as anhydrous ammonia. In the case of a spill of an aqueous ammonia solution, both soil and water can be polluted. Furthermore, there is the possibility of occurrence of a toxic cloud, which will depend on the mass of ammonia entering into the atmosphere and on the meteorological conditions. One of the key aspects is the ammonia evaporation rate from the pool.

Diverse authors have studied the evaporation of volatile compounds from liquid pools. Sutton (1934) developed a pioneering theoretical model to predict the evaporation rate from a plane surface as a function of wind speed. Mackay and Matsugu (1973) studied, both experimentally and theoretically, the evaporation of liquid hydrocarbon spills on land and water. Clewell (1983) performed experimental work on the evaporation of hydrazine from aqueous solutions spilled on ground. Other expressions were also proposed by Kawamura and Mackay (1987), who studied the evaporation of hydrocarbons (cyclohexane, n-pentane, n-hexane and toluene) with wind speeds ranging between 2.6 and 5.4 m s^{-1}. Brighton (1990) reported data on the evaporation of n-butane at temperatures below its boiling point and wind speeds ranging between 0.5 and 5.5 m s^{-1}. US EPA (1989) and Mikesell et al. (1991) studied the evaporation from multicomponent non ideal solutions. Oil spills evaporation –physics involved and mathematical modeling– was reviewed by Fingas (1995); this author (Fingas, 1998) also studied experimentally the evaporation from crude oil and petroleum products. Van den Bosch (2005) proposed a model to estimate the evaporation rate from a non-boiling pure liquid, which included the influence of the wind speed and the temperature.

* Corresponding author.
E-mail address: joaquim.casal@upc.edu (J. Casal).

https://doi.org/10.1016/j.jlp.2022.104750
Received 20 December 2021; Received in revised form 24 January 2022; Accepted 7 February 2022
Available online 12 February 2022

Heymes et al. (2013) published experimental data on the evaporation of several volatile organic compounds and water at wind speeds ranging between 1.6 and 4 m s^{-1}. Recently, Bubbico and Mazzarotta (2016) have analyzed 9 models by comparing them with a set of 73 experimental data on the evaporation of organic compounds, finding that for wind velocities higher than 1 m s^{-1} the model proposed by Heymes et al. (2013) gave the best estimates.

However, even if ammonia spills are important because of the risk associated essentially to its toxicity, rather few experimental data are still available. Mikesell et al. (1991) performed two experiments with ammonia aqueous solutions. Dharmavaram et al. (1994) analyzed the ammonia spills from a barge into water, taking into account the initial boiling but considering the later evaporation rate as essentially zero. Ye et al. (2008) studied experimentally the ammonia evaporation from aqueous solutions, analyzing the mass transfer coefficient behavior as a function of the ventilation rate and turbulence intensity. Galeev et al. (2013) proposed a mathematical model to estimate the toxic impact zones due to ammonia evaporation from aqueous solution spills.

In this communication, the evaporation of ammonia from aqueous solutions at different concentrations and under different wind speeds is analyzed, both experimentally and theoretically.

2. Experimental set-up

In order to study the influence of the main variables on the ammonia evaporation, an experimental installation was constructed. The air flowed through a duct (rectangular section, 220 mm × 100 mm), conveniently designed to minimize the turbulence, towards and from the evaporation chamber (chamber volume: 6.2 L) (Fig. 1). The air was sucked by a fan located downstream. In the evaporation chamber there was a thermally insulated tray (270 mm × 185 mm x 10 mm) which contained the ammonia solution. The tray was located over a digital weighing scale, which allowed the continuous registration of the solution weight by a data acquisition system (Field Point, National Instruments). The solution surface was parallel to the air stream and leveled in such a way to minimize turbulence. The initial concentration of ammonia in the tests was 29% in mass, the initial mass of solution was 180 g and its depth was 1 cm. The air speed ranged between 0.8 and 4.1 m s^{-1}, a range of special interest for risk analysis: at higher air speed the atmospheric dispersion is rather intense and the analysis of the toxic impact has no interest, and at lower speed the influence of wind is almost negligible.

The variables measured were the air speed, temperature and humidity, and the concentration, mass and temperature of the solution along the time. The mass in the tray was registered continuously. The ammonia concentration was measured approximately every minute or 1.5 min by taking a small sample and analysing it by refractometry. The temperature of air varied between 24 and 27 °C, and its relative humidity ranged between 53% and 55%. Air speed was measured at four different flowrates with a hot wire (TESTO 480) located at the evaporation chamber entrance, 1 cm above the liquid level; previously a detailed analysis of the speed profile over the cross section of the evaporation chamber was effectuated. The treatment of these data gave the following mean values above the cross section: 0.8 m s^{-1}, 1.6 m s^{-1}, 3.1 m s^{-1} and 4.1 m s^{-1}.

The air humidity was measured with an electronic hygrometer (TFA 30.5005). The ammonia concentration was determined by refractometry (Atego-Smart I). Finally, the amount of condensed water was determined from the difference between its initial and final mass. The initial mass of water was known and, as the mass and concentration of the solution were continuously registered (Sartorius BL-600), the amount of water in the solution at any moment could also be known.

3. Experimental results

3.1. Evaporation rate

The evaporation rate over a given area A of a spill can be predicted theoretically by the following expression (Kawamura and Mackay, 1987; Van den Bosch, 2005):

$$E = k \cdot A \cdot M \cdot P_{Tsol} / (RT_{sol}) \quad (1)$$

where k is the mass transfer coefficient (m/s) (which is a function of the air speed), A is the spill surface area (m^2) and P_{Tsol} is the vapor pressure of the chemical at the temperature of the liquid surface.

The velocity at which ammonia evaporates at a given temperature depends on the air speed. In Fig. 2 the percentage of solution mass loss in the vessel as a function of time is shown for the four air velocities. The

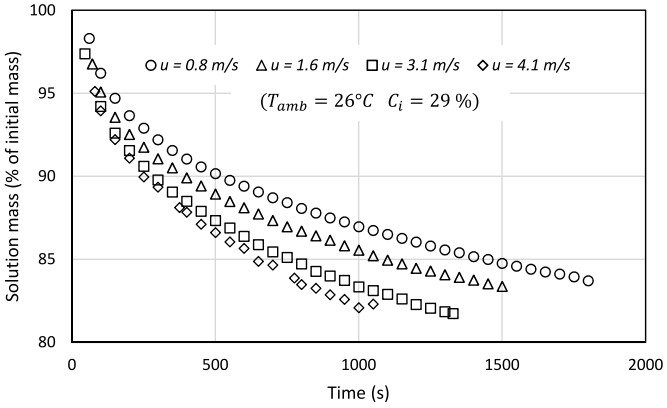

Fig. 2. Evolution of the solution mass due to evaporation of ammonia (and, from a certain moment, to water condensation) as a function of time and air speed.

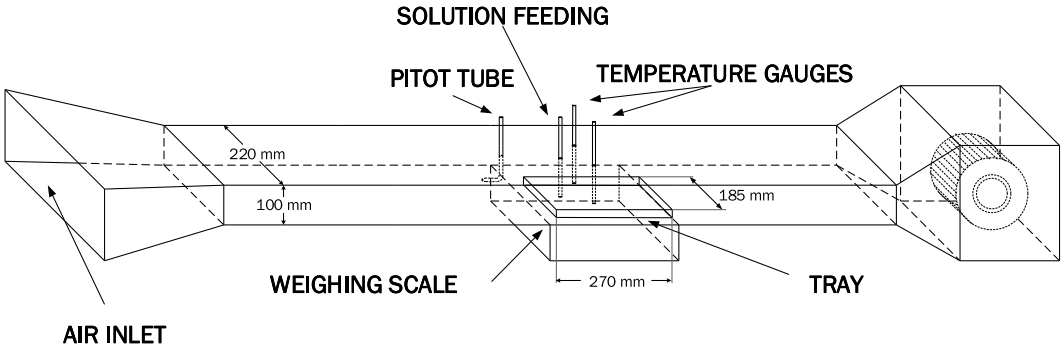

Fig. 1. Experimental set-up.

solution mass decreases quickly at the beginning of the test, indicating a high ammonia evaporation rate. Afterwards, the process proceeds more and more slowly due to the fact that the ammonia concentration in the solution and the temperature in the liquid (especially in the upper layer) decrease.

Higher air speeds imply higher evaporation rates. In Fig. 3 the evolution of the accumulated mass of evaporated ammonia is plotted for a given period of time, for the same air speeds and initial concentration solutions plotted in Fig. 2, showing the aforementioned influence of the variation of ammonia concentration and of the solution temperature.

The variation of the evaporation rate as a function of time has been plotted in detail in Fig. 4 for a given initial concentration. The evaporation rate is very high in the first moments and decreases quickly with time as the concentration of ammonia in the solution decreases: while after the first 1.5 min it is 0.12 g/s, half a minute later it has decreased to half this value.

The evolution of ammonia concentration, decreasing with time as this component evaporates, has been plotted in Fig. 5 for the different air speeds. The rate at which it decreases varies significantly with this variable, increasing with it.

3.2. Influence of the air speed on the evaporation rate

The air speed (wind) is an important variable in the event of an accidental spill, as it has an effect on both the velocity at which the volatile components evaporate and, also, together with the atmospheric stability, on the way in which the toxic cloud –in the present case, of ammonia– evolves and moves.

The influence of the air speed on the evaporation rate was analyzed by Sutton (1934) for the case of evaporation from a water pool. This author used the power law which establishes the variation of the wind velocity as a function of height, on the assumption that there is no velocity at the surface (1 and 2 indicating two different heights):

$$u_1 = u_2 \left(\frac{z_1}{z_2}\right)^{\frac{n}{2-n}} \tag{2}$$

And, for the mean rate of evaporation under steady state conditions:

$$E \propto u^{\frac{2-n}{2+n}} \tag{3}$$

Taking $n = 0.25$ for turbulent medium and average atmospheric conditions, Sutton (1934) proposed the following expression for the evaporation from pure liquids:

$$\frac{E_2}{E_1} = \left(\frac{u_2}{u_1}\right)^{\alpha} \tag{4}$$

With the approximate value $\alpha = 0.78$, which was in good agreement with experimental data on water evaporation. However, this coefficient

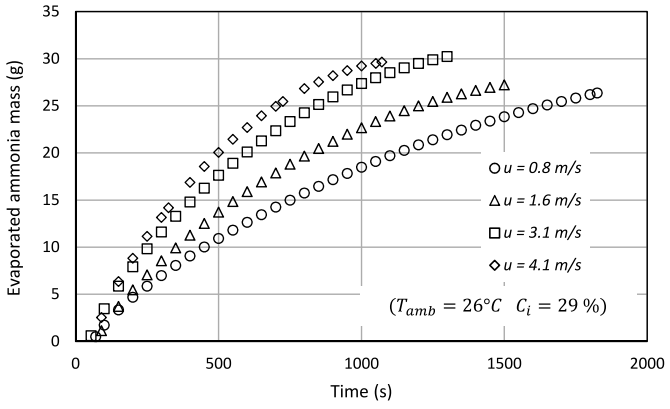

Fig. 3. Accumulated mass of evaporated ammonia as a function of time and air speed.

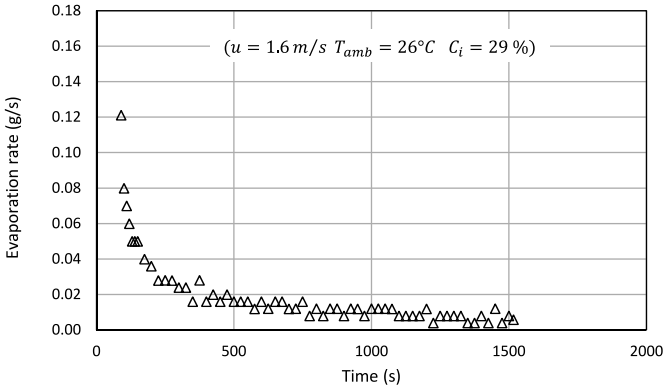

Fig. 4. Evolution of the evaporation rate as a function of time.

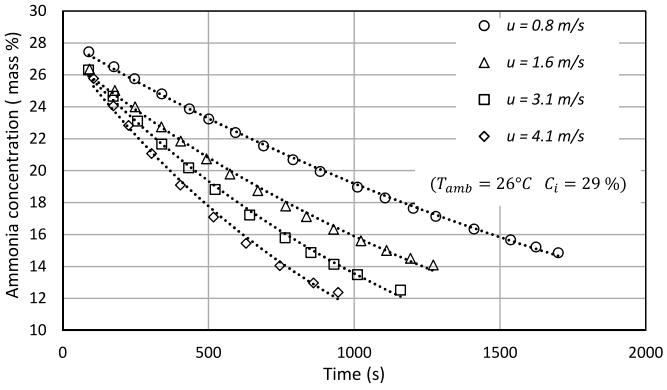

Fig. 5. Variation of ammonia concentration with time and air speed.

–and the n value– really changes with the atmosphere temperature profile, with the atmospheric stability class and with the surface roughness (urban or rural zone, or water). Furthermore, in the present case the spill is not that of a pure liquid and, as the ammonia concentration changes with time, it was not clear whether this expression could be applied; so, this point was analyzed.

The variation of ammonia vaporization rate as a function of air speed has been plotted for different ammonia solution concentrations in Fig. 6. These data were obtained as follows: for a given constant air speed, the ammonia concentration was measured throughout the test; at certain concentration values (25%, 23%, 21%, 19%, 17% and 15%, mass percentage), the evaporation rate was obtained from the values of concentration and solution mass. This was done for tests at the different air speeds. As evaporation was continuous during each test, the solution temperature varied (see Fig. 7), this introducing a light difference in the respective conditions of the experimental points. As the solution concentration increases the evaporation rate increases significantly. And at high concentrations (25% and 23%, Fig. 6-b) an important dispersion was registered due to the difficulty in the measurement of the concentration in that period of the tests.

From this figure it is clear that the evaporation rate increases with the ammonia concentration and with the air speed (corresponding to the evolution of ammonia concentration shown in Fig. 5). However, the relationship between the evaporation rate and the air speed changes with the solution concentration. Thus, the α value has been calculated for each case (Table 1):

According to these data, it seems therefore that Eq. (4), developed for pure liquids, should not be applied to the evaporation from ammonia aqueous solutions.

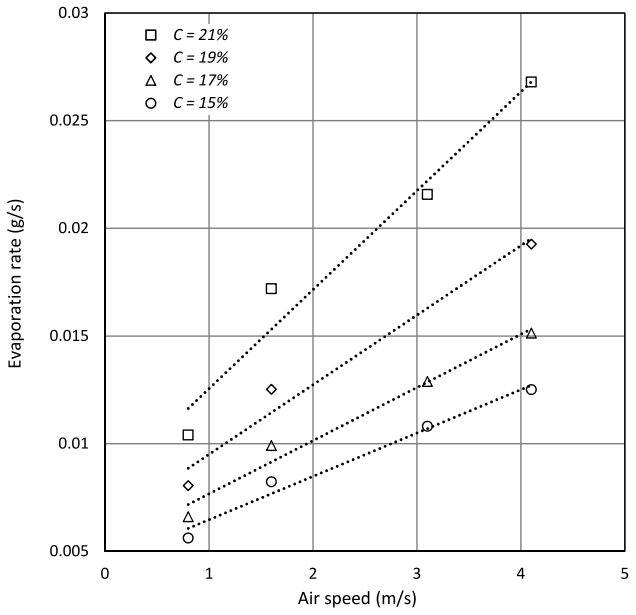

(a)

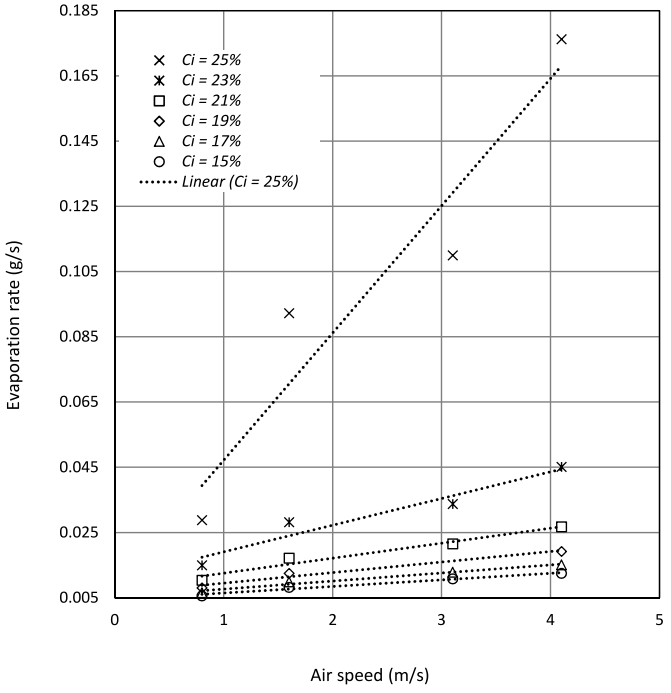

(b)

Fig. 6. Ammonia vaporization rate as a function of air speed for different ammonia concentrations (mass percentage) (initial temperature: 26 °C).

3.3. Evolution of temperature

An important aspect in the evaporation process is the evolution of the solution temperature. As evaporation proceeds, the solution is subjected to a cooling action, as the latent heat of evaporation is taken from the remaining liquid. Therefore, the cooling rate directly depends on the evaporation rate. It is higher during the first steps of the process and later decreases gradually as the pool temperature, the vapor pressure of ammonia, the ammonia concentration, and the vaporization rate decrease. The evolution of the solution temperature can be observed in Fig. 7 for the four air speeds.

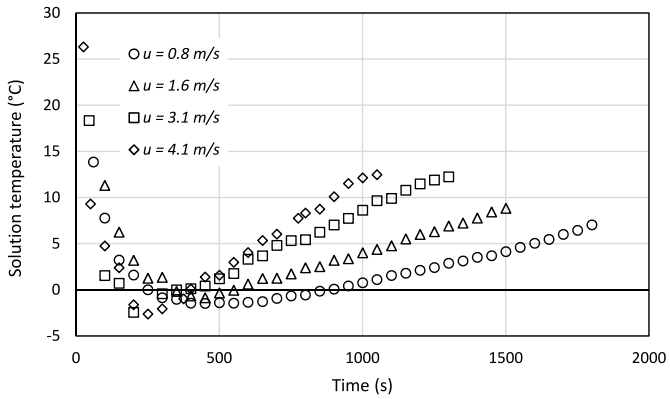

Fig. 7. Variation of the solution temperature as a function of time at different air speeds (T_{amb} = 26 °C, C_i = 29%).

Table 1
Calculated α values for different ammonia concentrations.

C, % mass	α
25	0.89
23	0.58
21	0.51
19	0.49
17	0.46
15	0.45

From Fig. 7 it can be seen that there is an important cooling of the remaining solution during the first minutes –corresponding to high ammonia vaporization rates–, with temperatures decreasing below 0 °C. After reaching a minimum value the temperature gradually increases during the rest of the tests, due to the condensation of water from the atmosphere. The time at which the minimum is reached decreases as the air speed increases. This is due to the fact that a) the ammonia vaporization rate is higher (stronger cooling of solution), and b) the higher water condensation rate that cooling originates, with the corresponding higher introduction of heat into the solution, reverses the trend of the temperature evolution sooner. This behavior is important as, in a real large-scale accidental spill; it will have an influence on the dynamics of the generation of a toxic cloud.

3.4. Water condensation

During most of the tests' duration, the evaporation of water from the aqueous solution was not possible due to the cooling effect in the upper liquid layer associated with the ammonia evaporation. However, as the temperature of this upper liquid layer decreased relatively quickly, it was soon lower than the air dew point; therefore, the inverse process (i.e., the condensation of water from the air humidity due to the low solution temperature) was confirmed. Fig. 8 shows the evolution as a function of time of the accumulated condensed water and condensation rate, respectively –starting from a certain moment– for a given air velocity.

This phenomenon must be considered to avoid an underestimation of the ammonia evaporation rate by overestimating the temperature decrease. The determination of the mass of water condensed during the whole process has been done by a mass balance, taking into account the initial mass of water, the concentration of ammonia and the variation of the total solution mass as a function of time.

The accumulated mass of condensed water increased from a certain moment as a function of time; while the condensation rate decreased as the solution temperature increased and approached the dew point of air.

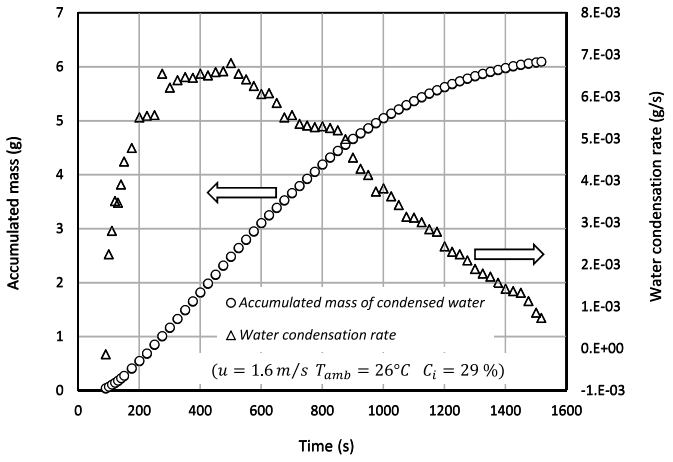

Fig. 8. Evolution of water condensation as a function of time.

Finally, after a certain time the mass of water in the tray kept constant, thus indicating that there was no more condensation.

Thus, during a certain time the solution undergoes simultaneously a heating effect due to the input of the latent heat of water condensation and a cooling effect originated by the output of the latent heat of ammonia evaporation (λ_w is approximately twice λ_{NH3}). The difference between both –heating and cooling– effects is important at the beginning (Fig. 9) and decreases progressively as the solution temperature increases and the ammonia concentration and evaporation rate decreases.

4. Process phases

During the evaporation process, the solution temperature changes significantly, being influenced by the ammonia evaporation rate, the air speed, the heat transfer from the environment, and the condensation of water. This phenomenon can be explained in terms of the following phases (Corruchaga and Casal, 2015) (Fig. 10):

The three phases in the evaporation process, with of course a smooth transition between them, are:

Phase I). There is a high ammonia evaporation rate, which implies a significant decrease in the enthalpy of the solution (the evaporation latent heat of ammonia is taken from the solution) with the associated decrease of its temperature.

Phase II). Due to the progressive reduction of the ammonia concentration and of the solution temperature, the ammonia evaporation rate decreases; this implies that the cooling velocity of the solution decreases as well. Simultaneously, due to the low temperature of the solution, the heat transfer rate from the environment to it –from the air essentially by

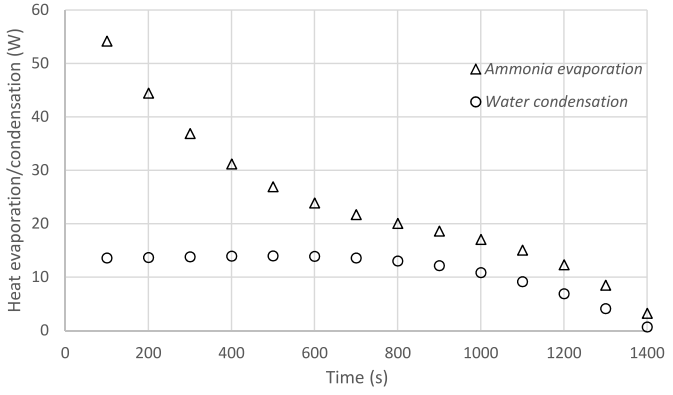

Fig. 9. Evolution of cooling and heating effects as a function of time ($u = 1.6$ m s^{-1}).

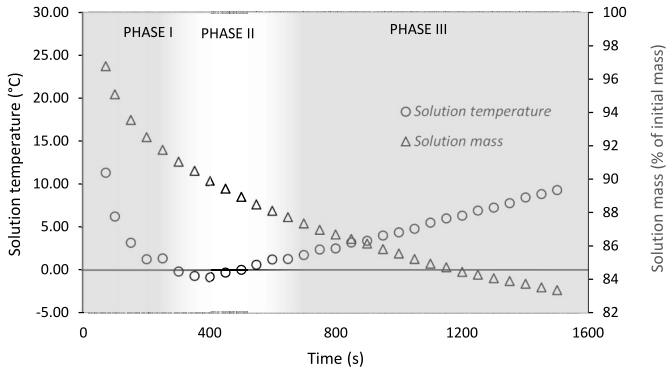

Fig. 10. The three phases observed in the evaporation process (air speed: 1.6 m s^{-1}; C_i: 29 mass %).

convection, and perhaps also from the vessel by conduction– increases. Furthermore, some water from the air condenses on the cold solution, releasing its condensation latent heat. The temperature of the solution starts to increase. This situation leads to the existence of a minimum value of the solution temperature. The time at which this minimum value is reached decreases lightly as the air speed increases.

Phase III). Ammonia evaporation rate keeps decreasing while the environment heats more and more the solution, and some water keeps condensing. As a consequence, the temperature of the solution progressively rises towards that of the air stream.

The existence of these three different phases can be important from the point of view of analyzing the risk associated with the possible generation of a toxic cloud in the event of a toxic solution spill, as it will establish the kinetics of the toxic cloud generation.

5. Enthalpy balance

The evolution of the temperature of the solution can be determined from the different contributions: (i) cooling due to ammonia evaporation; (ii) cooling due to the initial water evaporation; (iii) heating from the surroundings; and (iv) heating due to the condensation of water from the atmosphere.

It has been assumed that the evaporation of water in the first moments is negligible. Then, with a simple approach based on that proposed by Mackay and Matsugu (1973), the following enthalpy balance can be applied to establish the evolution of the solution temperature as a function of time:

$$\frac{dT}{dt} = \frac{(Q_{amb} + Q_{cond} - Q_{evap})}{m_{sol} \cdot Cp_{sol}} \tag{5}$$

In this expression the contribution of the condensation of water from a certain moment, due to the low solution temperature, has been included.

The different contributions have been calculated as follows. Heat transfer from the air:

$$Q_{amb} = A \cdot U_{air-sol} \cdot (T_{air} - T_{sol}) \tag{6}$$

where A is the solution surface area, T_{air} and T_{sol} are the temperatures of air and of the solution upper layer, respectively, and $U_{air\text{-}sol}$ is the overall heat transfer coefficient air-liquid, which can be estimated from the heat and mass transfer analogy (Kawamura and Mackay, 1987):

$$U_{air-sol} = k \cdot \rho_{air} \cdot C_{pa} \cdot \left(\frac{Sc}{Pr}\right)^{0.67} \tag{7}$$

where k is the mass transfer coefficient, ρ_{air} is the air density, C_{pa} is the specific heat of air, Sc is the Schmidt number in the air phase and Pr is the Prandtl number.

The mass transfer coefficient, k, was calculated by Mackay and

Matsugu (1973) with the following expression for the evaporation from hydrocarbon spills:

$$k = 0.0048 * u^{0.78} * X^{-0.11} * Sc^{-2/3} \quad (8)$$

in which u is the air velocity (m s^{-1}), its exponent being the one proposed by Sutton (1934) by average atmospheric conditions, X is the length of the evaporation pool (m) and the constant 0.0048 has units ($m^{0.33}$ $s^{-0.22}$). This expression was proposed just for situations with wind; it should not be applied for very volatile liquids in calm air situations, as it predicts no evaporation.

It can be assumed that k is a function of D, u, ρ and μ. The variable X was not included, as its influence on the air turbulence would be restricted just to a small zone on the upwind border of the spill. A dimensional analysis gives then the following expression:

$$k = f\left(u, \frac{\mu}{\rho D}\right) = f(u,\ Sc) = ct \cdot u^{\beta} \cdot Sc^{\gamma} \quad (9\text{-a})$$

In which the constant and the exponents β and γ must be obtained from experimental data. In the present work, the value of k has been calculated for the diverse air velocities and solution ammonia concentrations (Fig. 11).

From Fig. 11 the exponent of u in Eq. (9-a) corresponding to the experimental data and conditions has been obtained, 0.57. As all tests were performed at ambient temperature, which did not change much, the exponent of the Schmidt number could not be modified, and that of Eq. (8) has been taken, together with the value of the constant. Therefore, finally the expression for k was:

$$k = 0.0048 * u^{0.57} \cdot Sc^{-\frac{2}{3}} \quad (9\text{-b})$$

The validity of this new expression has been checked by comparing the values of k obtained with it with those obtained from the theoretical expression (1) in which the experimental value of the evaporation rate was introduced (Fig. 12). The result can be considered satisfactory.

The heat lost from the solution due to the ammonia evaporation can be calculated by:

$$Q_{evap} = E \cdot \lambda_{NH_3} \quad (10)$$

And the ammonia evaporation rate can be estimated by introducing Eq. (9-b) in the expression proposed by Van den Bosch (2005):

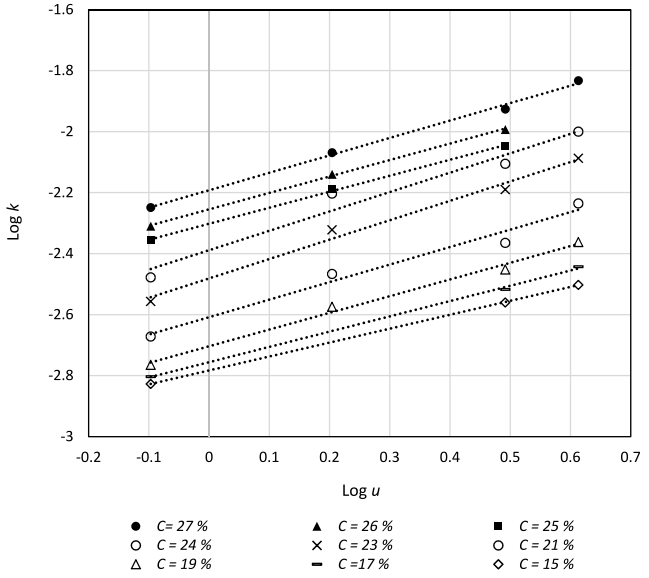

Fig. 11. Mass transfer coefficient, k, as a function of air velocity (u, m/s) and solution concentration (mass %).

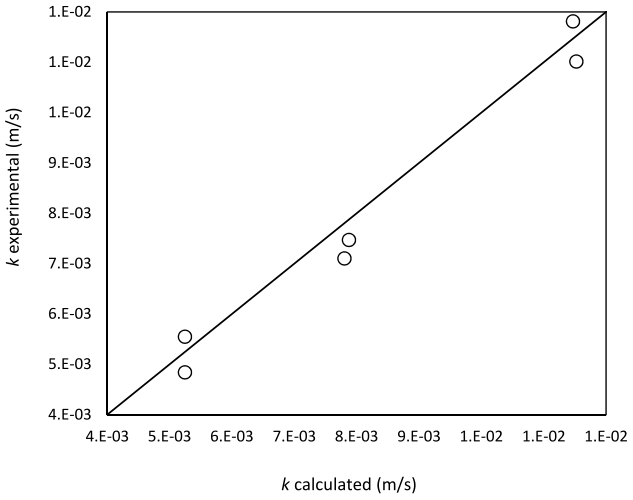

Fig. 12. Comparison of k values obtained with Eq. (9-b) with those predicted from the experimental data by Eq. (1).

$$E = 0.0048 \cdot u^{0.57} \cdot A \cdot M_{NH_3} \cdot \frac{1}{R \cdot T_{sol}} \cdot P_{amb} \cdot \log\left(1 + \frac{P_{NH3} - P_0}{P_{amb} - P_{NH_3}}\right) \quad (11)$$

Finally, the heat gained by the solution due to the condensation of water from the air humidity (condensing at a rate of W_w in kg/s) can be calculated by:

$$Q_{cond} = W_w \cdot (H_w - h_w) = W_w \cdot (\lambda_w + Cp_v\ (T_{air} - T_{sol}) \quad (12)$$

where H_w and h_w are the enthalpy of vapor and liquid water, respectively, λ_w is the condensation latent heat of water and Cp_v is the specific heat of water vapor.

This condensation implies a progressive increase of the temperature of the solution. This set of expressions have been solved with Matlab R2018b ® to predict the evolution of the solution temperature and of the evaporation rate as a function of time. This can be important in the event of an accidental spill, as it can play an important role in the possible generation of a toxic cloud.

6. Comparison of calculated and experimental values

The results obtained from these expressions (Eq. (5) - (12)) have been compared with the experimental values. Fig. 13 shows the four sets of data for the evolution of the solution temperature as a function of time and of air speed.

The trend of the four sets of data is similar and the agreement between the experimental values and those predicted by the model is relatively good, even though there is a certain difference which increases with the air speed and with time. At low air speed (0.8 m s^{-1}) the model overpredicts slightly the solution temperature in the first phase, corresponding to high evaporation rates; this overprediction decreases as air speed increases (1.6 m s^{-1}). At higher air speeds (3.1 m s^{-1}) the calculated values in Phase III, when there is water condensation from the atmosphere, are slightly lower than the experimental ones, this difference increasing at the highest speed (4.1 m s^{-1}).

Finally, the experimental data and the corresponding predicted values of the ammonia evaporation rate as a function of time for a given case have been plotted in Fig. 14. There is again a certain difference between both sets of values: in Phase I the model slightly underpredicts the evaporation rate, the difference decreasing with time. After the first 3 min it predicts values very close to the experimental ones even though slightly higher; as a whole, the agreement between both sets of values can be considered acceptable.

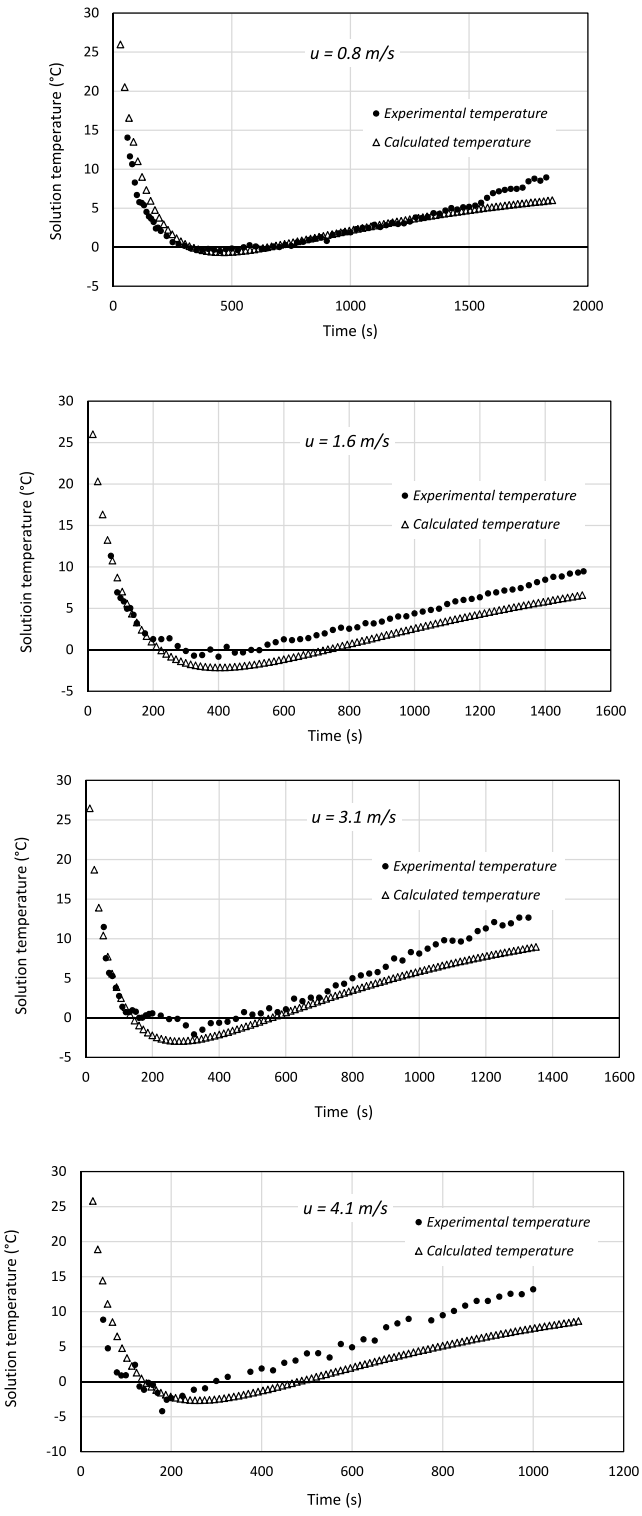

Fig. 13. Evolution of the solution temperature as a function of time for the four air speeds: comparison of the calculated values and the experimental data (T_{amb} = 26 °C, C_i = 29% mass).

7. Conclusions

The evaporation of ammonia from an aqueous spill, which depending on the flow rate and the meteorological conditions can originate a toxic cloud, is strongly influenced by the ammonia concentration in the spilled solution, by the temperature and by the wind speed. The initial evaporation rate is very high, decreasing quickly in the first minutes and afterwards progressively as the ammonia concentration and the solution temperature decrease. The evaporation rate increases with the air speed and with the solution concentration. The temperature of the solution decreases as evaporation proceeds, reaching values lower than 0 °C and increasing later due to the condensation of water from atmospheric humidity.

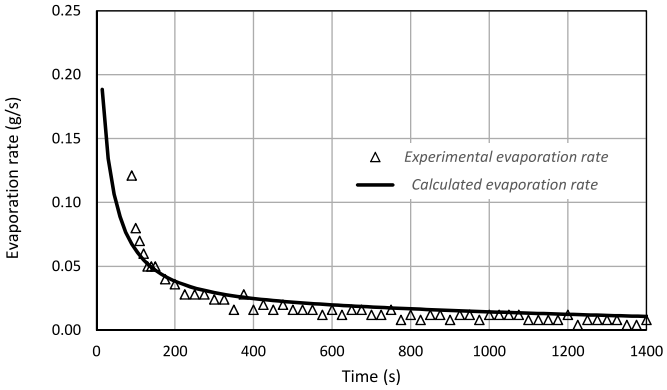

Fig. 14. Ammonia evaporation rate: comparison between predicted and experimental data (u = 1.6 m s^{-1}, C_i = 29%, T_{amb} = 26 °C).

As a whole, three phases have been observed: I) A first one with high ammonia evaporation rate and a clear decrease in the solution temperature. II) A second one in which the ammonia evaporation rate decreases; after reaching a minimum value, the solution temperature starts to increase due to the condensation of water from air humidity. III) And a third one, in which ammonia evaporation rate decreases more and more and the solution temperature keeps increasing due to the condensation of water; in this third phase the water condensation rate decreases with time as the solution temperature slowly increases. This behavior –which does not include any initial ammonia boiling or flash in the first moments of the release– is very interesting from the point of view of the dynamics of the possible generation and evolution of a toxic cloud in the event of an accidental spill.

A simple mathematical model has been proposed to describe the process. Although it is related to other models previously published in the literature (most of them concerning the evaporation of hydrocarbons), it has the novelty of including the condensation of water from the atmospheric air humidity. Even though the comparison of the predicted values with the experimental ones shows a certain scattering, it could be useful to predict the source term (ammonia evaporation rate) in the event of an accidental spill in an industrial plant or during transportation, especially at low wind speeds in which the risk associated to the formation of a toxic cloud is higher.

Author contribution statement

All authors contributed to all sections, and with the same workload.

Declaration of competing interest

The authors declare that they have no known competing financial interests or personal relationships that could have appeared to influence the work reported in this paper.

Acknowledgements

A. P. gratefully acknowledges financial support of the Royal Society as a Postdoctoral Newton International Fellowship.

Notation

A	solution surface area (m^2)
C	ammonia concentration (mass %)
C_i	initial ammonia concentration (mass %)
Cp_a	specific heat of air (kJ kg^{-1} $°C^{-1}$)
Cp_{sol}	specific heat of solution (kJ kg^{-1} $°C^{-1}$)
Cp_v	specific heat of water vapor (kJ kg^{-1} $°C^{-1}$)
D	diffusivity of ammonia in air (m^2 s^{-1})
E	ammonia evaporation rate (g s^{-1})
h_w	enthalpy of liquid water at the temperature of the solution (kJ kg^{-1})
H_w	enthalpy of water vapor at the temperature of air (kJ kg^{-1})
k	mass transfer coefficient (m s^{-1})
l	tray length (m)
m_{sol}	mass of solution (kg)
M_{NH3}	molecular weight of ammonia (g/mol)
n	constant in the wind velocity power law, Eqs. (2) and (3) (–)
P_{amb}	atmospheric pressure (Pa)
P_{NH3}	ammonia vapor pressure at the solution surface (Pa)
P_0	ammonia vapor pressure in the atmosphere (Pa)
Pr	Prandtl number (–)
P_{Tsol}	Vapor pressure of the chemical at the solution surface temperature (Pa)
Q_{amb}	heat gained by the solution from the surroundings (kW)
Q_{cond}	heat gained by the solution due to the condensation of water (kW)
Q_{evap}	heat lost by the solution due to ammonia evaporation (kW)
R	ideal gas constant (m^3 Pa mol^{-1} K^{-1})
Sc	Schmidt number (–)
t	time (s)
T	temperature (°C)
T_{air}	temperature of air (°C)
T_{amb}	ambient temperature (°C)
T_{sol}	temperature of the solution surface (°C)
u	air speed (m s^{-1})
$U_{air\text{-}sol}$	overall heat transfer coefficient from air stream to liquid surface (kW m^{-2} $°C^{-1}$)
W_w	water condensation rate (kg s^{-1})
X	length of the evaporation chamber (m)
z	height (m)

Greek letters

α	exponent of wind velocity in the evaporation rate expression, Eq. (4) (–)
β	exponent of the air speed in Eq. (9-a)
γ	exponent of Sc in Eq. (9-a)
λ_{NH3}	vaporization latent heat of ammonia at the solution surface temperature (kJ kg^{-1})
λ_w	condensation latent heat of water at the solution surface temperature (kJ kg^{-1})
μ	dynamic viscosity (kg m^{-1} s^{-1})
ρ_{air}	air density (kg m^{-3})

References

Brighton, P.W.M., 1990. Further verification of a theory for mass and heat transfer from evaporating pools. J. Hazard Mater. 23, 215–234.

Bubbico, R., Mazzarotta, B., 2016. Predicting evaporation rates from pools. Chem. Eng. Trans. 48, 49–54.

Clewell, H.J., 1983. A Simple Method for Estimating the Source Strength of Spills of Toxic Liquids. Energy Systems Laboratory ESL-TR-83-03.

Corruchaga, A., Casal, J., 2015. Evaporation of ammonia from aqueous solutions spills. In: Proceedings of the 14th International Conference on Environmental Science and Technology. https://cest2015.gnest.org/papers/cest2015_01370_oral_paper.pdf.

Dharmavaram, S., Tilton, J.N., Gradner, R.J., 1994. Fate and transport of ammonia spilled from a barge. J. Hazard Mater. 37, 475–487.

Fingas, M.F., 1995. A literature review of the physics and predictive modelling of oil spill evaporation. J. Hazard Mater. 42, 157–175.

Fingas, M.F., 1998. Studies on the evaporation of crude oil and petroleum products. II. Boundary layer regulation. J. Hazard Mater. 57, 41–58.

Galeev, A.D., Salin, A.A., Ponikarov, S.I., 2013. Consequence analysis of aqueous ammonia spill during computational fluid dynamics. J. Loss Prev. Process. Ind. 26, 628–638.

Heymes, F., Aprin, L., Bony, A., Forestier, S., Cirocchi, S., Dusserre, G., 2013. An experimental investigation of evaporation rates for different volatile organic compounds. Process Saf. Prog. 32, 193–198.

Kawamura, P.I., Mackay, D., 1987. The evaporation of volatile liquids. J. Hazard Mater. 15, 343–364.

Mackay, D., Matsugu, R.S., 1973. Evaporation rates of liquid hydrocarbon spills on land and water. Can. J. Chem. Eng. 51, 434–439.

Mikesell, J.L., Buckland, A.C., Diaz, V., Kives, J.J., 1991. Evaporation of contained spills of multicomponent non ideal solutions. In: Proceedings of the International Conference and Workshop on Modelling and Mitigating the Consequences of Accidental Releases of Hazardous Materials, pp. 103–123. May 20-24: New Orleans, Louisiana.

Ronza, A., Carol, S., Casal, J., 2006. Assessing the number of injured people in major accidents. J. Hazard Mater. 133, 46–52.

Sutton, O.G., 1934. Wind structure and evaporation in a turbulent atmosphere. Proc. Roy. Soc. Lond. A 146, 701–722.

Toscano, G., Corruchaga, A., Pastor, E., Bonvicini, S., Palacios, A., Casal, J., 2022. Risk analysis of ammonia pipeline transport. EMChIE (accepted).

U. S. Department of Transportation. U. S. Environmental Protection Agency, 1989. Handbook of Chemical Hazard Analysis Procedures. Federal Emergency Management.

Van den Bosch, 2005. C. J. H. Pool evaporation. In: Van den Bosh, C.J.H., Weterings, R.A. (Eds.), Methods for the Calculation of Physical Effects CPR 14E ("Yellow Book"), third ed. Ministerie van Verkeer en Waterstaat, The Hague.

Ye, Z., Zhang, G., Li, B., Strom, J.S., Tong, G., Dahl, P.J., 2008. Influence of airflow and liquid properties on the mass transfer coefficient of ammonia in aqueous solutions. Syst. Eng. 100, 422–434.